G-quadruplex DNA motifs in the malaria parasite *Plasmodium falciparum* and their potential as novel antimalarial drug targets

Running title: G-quadruplexes in *Plasmodium falciparum*

Authors

Lynne M. Harris[1a], Katelyn R. Monsell[1a], Florian Noulin[1], M. Toyin Famodimu[1], Nicolas Smargiasso[2], Christian Damblon[2], Paul Horrocks[1,3], Catherine J. Merrick[1*]

Affiliations & Contact Information

[1]Centre for Applied Entomology and Parasitology, Faculty of Natural Sciences, Keele University, Keele, Staffordshire, ST55BG, UK;

[2]Molecular Systems Research Unit, University of Liege, Liege, Belgium;

[3]Institute for Science and Technology in Medicine, Keele University, Keele, Staffordshire, ST55BG, UK.

*Corresponding author:

c.merrick@keele.ac.uk (CJM)

Tel: (+44) 1782 734111

[a]These authors contributed equally to this work

KEYWORDS

Malaria, *Plasmodium falciparum*, G-quadruplex, Quarfloxin.

ABSTRACT

G-quadruplexes are DNA or RNA secondary structures that can be formed from guanine-rich nucleic acids. These four-stranded structures, composed of stacked quartets of guanine bases, can be highly stable and have been demonstrated to occur *in vivo* in the DNA of human cells and other systems, where they play important biological roles, influencing processes such as telomere maintenance, DNA replication and transcription, or in the case of RNA G-quadruplexes, RNA translation and processing. We report for the first time that DNA G-quadruplexes can be detected in the nuclei of the malaria parasite *Plasmodium falciparum*, which has one of the most A/T-biased genomes sequenced and therefore possesses few guanine-rich sequences with the potential to form G-quadruplexes. We show that despite this paucity of putative G-quadruplex-forming sequences, *P. falciparum* parasites are sensitive to several G-quadruplex-stabilizing drugs, including quarfloxin which previously reached Phase-2 clinical trials as an anticancer drug. Quarfloxin has a rapid initial rate of kill and is active against ring stages as well as replicative stages of intraerythrocytic development. We show that several G-quadruplex-stabilising drugs including quarfloxin can suppress the transcription of a G-quadruplex-containing reporter gene in *P. falciparum*, but that quarfloxin does not appear to disrupt the transcription of rRNAs, which was proposed as its mode of action in both human cells and trypanosomes. These data suggest that quarfloxin has potential for repositioning as an antimalarial with a novel mode of action. Furthermore, G-quadruplex biology in *P. falciparum* may present a target for development of other new antimalarial drugs.

IMPORTANCE

The malaria parasite *Plasmodium falciparum* has historically become resistant to every antimalarial drug deployed, leading to a constant demand for new drugs and novel molecular targets for their development. G-quadruplex DNA motifs have been studied as a possible target for anti-cancer drugs, yielding an abundance of G-quadruplex-binding compounds, several of which have undergone clinical trials although none has yet reached the clinic. Here, we examine the existence and function of G-quadruplex motifs in the *P. falciparum* genome, and investigate the possibility of repurposing G-quadruplex-binding compounds as novel antiplasmodial agents. We show that G-quadruplex DNA motifs can be detected in the *P. falciparum* genome, and can modulate expression of a G-quadruplex-containing reporter gene. We also show that one G-quadruplex-binding drug, which previously underwent Phase-2 clinical trials, is potent and fast-acting against the intraerythrocytic stages of the parasite *in vitro*. G-quadruplexes thus constitute a possible new drug target in *P. falciparum.*

INTRODUCTION

Protozoan *Plasmodium* parasites are the causative agents of human malaria, a disease responsible for widespread morbidity and about half a million deaths each year (1). Most malaria deaths are caused by the species *P. falciparum*, although five other *Plasmodium* species also infect humans*. P. falciparum* has one of the most A/T-biased genomes ever sequenced, at ~81% A/T (2). Interestingly, not all *Plasmodium* species share this feature: the genome of the second major human malaria parasite, *P. vivax*, is only ~58% A/T, whereas the genome of the well-studied rodent malaria species, *P. berghei,* is more similar to *P. falciparum* at ~78% A/T (3, 4).

The A/T-biased genome in species like *P .falciparum* results in an extreme paucity of guanine-rich sequences, and hence of putative G-quadruplex forming sequences, or 'PQSs' (5). The G-quadruplex is one of many non-double-helical secondary structures that can be formed by DNA, alongside triplexes, hairpins, etc. To form an intramolecular G-quadruplex motif, four tracts of at least three guanines are required in close proximity, in order to form the type of structure shown in Figure 1A (6). Genome sequences can thus be mined for PQSs by searching for the consensus sequence $G_3 N_{1-7} G_3 N_{1-7} G_3 N_{1-7} G_3$ (7), although there is increasing evidence that G-quadruplexes may also fold with longer loops between the guanine tracts, with non-guanine 'bulges', and in 'inter-molecular' modes that involve both the sense and antisense strands of a DNA sequence (8, 9). Nevertheless, when the *P. falciparum* genome was analysed for conventional intramolecular PQSs, only 80 were found in genes or intergenic regions (5, 10). This translates to only one PQS per ~300kb of the non-telomeric *P. falciparum* genome, compared to an average of

one PQS per kb in the human genome (7). Several hundred PQSs were also found in the *P. falciparum* telomeres, which have the repeat sequence GGGTT(T/C)A and are inherently able to form G-quadruplexes (11, 12). Predicting the 'expected' PQS density of a given genome is not straightforward due to variable genome composition and biased base dyad frequencies, but under the simplest predictive algorithm (a Bernoulli stream of random bases at 81% A/T), a genome with the size and composition of *P. falciparum* contains no PQSs at all (5), therefore the maintenance of PQSs in specific genomic regions is likely to be biologically functional.

G-quadruplexes can have many important biological roles, including regulating telomere structure (13), inhibiting gene transcription (14) and promoting recombination, probably via stalling of RNA polymerases and replicative polymerases respectively (15, 16). In *P. falciparum* we have recently shown that PQSs are primarily clustered within the coding sequence or upstream of the major virulence gene family *var*, and that mitotic recombination events amongst *var* genes are strongly spatially associated with PQSs (5), so one role for G-quadruplexes in *P. falciparum* could be to promote the generation of *var* gene diversity. Here, we set out to establish experimentally whether G-quadruplexes are more broadly important for the biology of *P. falciparum*. If so, then interfering with G-quadruplex metabolism might be expected to affect the growth of the parasite and this would raise the possibility of repositioning G-quadruplex-binding compounds as antimalarial drugs. Many G-quadruplex-binding compounds have been developed in recent years, primarily as anticancer agents because several oncogenes such as c-*myc* are controlled by G-quadruplexes (14) and G-quadruplexes are also involved in telomere regulation (13). Thus, drugs that interfere with these processes can affect the viability of cancer cells more severely than normal cells. Similarly to rapidly-dividing

cancer cells, all single-celled eukaryotic pathogens must maintain their telomeres in order to survive as they replicate within their hosts, so telomere disruption would be one possible avenue for antimalarial activity of G-quadruplex-binding compounds. In fact, some such compounds have already been shown to bind to the *P. falciparum* telomere repeat (11). Alternatively, antimalarial activity might be achieved by disrupting the transcription or translation of essential G-quadruplex-containing genes, or by inducing a DNA damage response to G-quadruplex-stalled replication forks.

In addition to the established potential of G-quadruplex-binding drugs as anticancer agents, a precedent for their potential as anti-parasitic agents was recently published. Rudenko and co-workers, in the course of investigating RNA polymerase I inhibitors for their potency against *Trypanosoma brucei,* showed that the G-quadruplex-binding fluoroquinolone compound quarfloxin is trypanocidal with an IC_{50} of only 155nM (17). Quarfloxin disrupts RNA polymerase I activity by binding to G-quadruplexes in repetitive rRNA genes in the nucleolus, disrupting their physiological interaction with nucleolin and ultimately preventing rRNA transcription (18, 19). Cancer cells are hypersensitive to RNA polymerase I disruption (20) so quarfloxin was originally tested against neuroendocrine tumours and leukaemias but it was found to have poor bioavailability and to accumulate particularly in blood cells (21). This latter property may have reduced its effectiveness against solid tumours but it raised the possibility of targeting intra-erythrocytic malaria parasites instead. We have tested this concept, showing that quarfloxin is indeed a potent and fast-acting antiplasmodial compound *in vitro*, but that its mode of action is probably different from that demonstrated on human cells and trypanosomes.

RESULTS

G-quadruplexes can be detected in P. falciparum nuclei

The existence of G-quadruplexes in the *P. falciparum* genome has been predicted bioinformatically (5, 10) and PQSs from this genome have been shown to fold into G-quadruplexes *in vitro* (10, 11). To visualise G-quadruplex structures in cultured cells, structure-specific antibodies can be used, as demonstrated in mammalian cells (22-24) and ciliate macronuclei (25). Using immunofluorescence microscopy, we tested whether the G-quadruplex-specific antibody IH6 (24) could similarly recognise G-quadruplexes in *P. falciparum*. Clear nuclear staining was seen in all intraerythrocytic parasite stages (Fig .1B) and DNase treatment abolished this staining (but not the staining of a parasite protein, ERD2, used as a control). RNase treatment, by contrast, had no observable effect (Fig. 1C). A second independent G-quadruplex-specific antibody, BG4 (23), also gave comparable nuclear staining (Fig S1). G-quadruplex structures in DNA therefore appear to be consistently present during *P. falciparum* intra-erythrocytic development.

G-quadruplex-stabilising drugs inhibit the growth of blood-stage malaria parasites

If the G-quadruplexes detected in *P. falciparum* are important for parasite biology, G-quadruplex stabilisation might be expected to affect the growth of the parasite. We therefore tested the effect of several G-quadruplex-stabilising compounds on the *in vitro* growth of *P. falciparum* in a standard 48-hour assay encompassing one complete parasite growth cycle (26). The antiplasmodial potency of the compounds N-methyl-mesoporphyrin IX (NMM) (27, 28), 5,10,15,20-tetra-(N-methyl-4-pyridyl)porphine (TMPyP4) (29) and quarfloxin (18) varied widely, with EC_{50} values

ranging from 114nM for quarfloxin to 84μM for NMM (Fig. 2A). This variation could be due to the compounds having different G-quadruplex-stabilising capacities or varying affinities for different G-quadruplex isoforms, but it could also be due to off-target effects (particularly given the high EC_{50} values determined for some of the compounds). Therefore, to focus on G-quadruplex-binding properties alone, we directly compared the antimalarial potency of one of the compounds, TMPyP4, with a closely matched analogue, TMPyP2, which is structurally very similar but has a markedly lower G-quadruplex affinity via an alternative binding mode (30). Parasite growth was affected ~ 18-fold more severely by TMPyP4 than by TMPyP2, suggesting that unimpeded G-quadruplex metabolism does have an important role in the healthy growth of parasites. Furthermore, the most potent antiplasmodial activity in our panel of drugs was detected in quarfloxin, a drug that has already reached Phase-2 clinical trials.

Factors affecting the viability of a compound as a potential antimalarial drug include not only the EC_{50} but also the rate of kill. Therefore, to further define the antiplasmodial activities of the G-quadruplex-stabilising compounds, their initial rates of kill were determined in trophozoite intraerythrocytic stages using the bioluminescence relative rate of kill (BRRoK) assay (31). This assay uses a *P. falciparum* clone genetically engineered to express a luciferase reporter gene under a trophozoite-specific promoter. Thus it can determine the concentration-dependent effect of a drug upon cell viability, by measuring the bioluminescence signal from the rapidly turned-over luciferase protein. The loss of bioluminescence is benchmarked against the loss caused by a range of antimalarial compounds with well-defined rate of kill dynamics; shown here as dihydroartemisinin > chloroquine > mefloquine > atovaquone (Fig 2B). Comparison of the loss of bioluminescence signal after 6 hours

of exposure to the G-quadruplex-stabilising compounds indicated a range of initial RoK, with the rank order: NMM > quarfloxin > TMPyP2 = TMPyP4 (Fig 2C). Relative to the antimalarial benchmarks, NMM exhibited a rapid cytocidal activity comparable to chloroquine; while quarfloxin was comparable to mefloquine at low concentrations and to chloroquine and dihydroartemesinin at high concentrations. Neither TMPyP2 nor TMPyP4 showed cytocidal activity during this 6-hour assay, potentially reflecting a lag-phase in their antiplasmodial activity (31). These data were consistent with BRRoK data generated in a second strain of *P. falciparum* carrying the same luciferase reporter construct (Fig. S2A, B) and EC_{50} values were likewise consistent across two different strains (Fig. S2C).

Quarfloxin targets all stages of the erythrocytic lifecycle, including the ring stage

Whilst G-quadruplexes can be detected at all stages of the intraerythrocytic cycle (Fig. 1B), the BRRoK assay only effectively measures rate of kill in trophozoites because the luciferase reporter gene used in this assay is expressed from a trophozoite-specific promoter (31). We therefore investigated the cytocidal effect of quarfloxin and NMM at other stages of the erythrocytic cycle by visual assessment of synchronised parasites together with flow-cytometric measurement of their DNA content. Dead parasites do not synthesise new DNA, they tend to become visibly pyknotic and do not progress to the next morphological stage at the expected timepoint. Figure 3 shows that quarfloxin was highly active against ring stages, preventing the great majority of them from ever progressing to trophozoites. It was almost equally active against trophozoites, but less active against schizonts, a substantial proportion of which reinvaded to rings before dying in the next cycle. By

contrast, although NMM appeared to be more potent than quarfloxin in the BRRoK assay, it showed little activity against rings, which were largely able to progress to trophozoites (Fig.S3). Corroborating the BRRoK assay, however, NMM was potent against trophozoites and prevented them from progressing to schizonts. These data point to different modes of antiplasmodial action for these two G-quadruplex-binding compounds.

Quarfloxin does not affect telomere maintenance

G-quadruplex-binding compounds may kill cells via a variety of molecular mechanisms, including inducing telomere dysfunction, disrupting DNA replication or disrupting the transcription of important genes (such as rRNAs, as discussed in the introduction). The disruption of DNA replication seemed an unlikely mode of action for quarfloxin because it was highly potent against pre-replicative rings, but the disruption of gene transcription or an acute response to telomere dysfunction were both possibilities. We therefore investigated these possible mechanisms, starting with the possibility of telomere dysfunction because the great majority of the PQSs in the *P. falciparum* genome are found in telomere repeats (10). Parasites were grown in relatively low levels of quarfloxin (120nM, ~EC_{50}) that could be tolerated for up to 15 growth cycles, but no evidence of telomere shortening or lengthening was detected by telomere restriction-fragment Southern blotting after longterm exposure to quarfloxin (Fig. S4).

The mode of action of quarfloxin may involve deregulated expression of PQS-containing genes

To investigate the possibility that transcription of essential G-quadruplex-containing genes was deregulated by quarfloxin, we assessed the transcription of a validated G-quadruplex-containing reporter gene and also the transcription of rRNA genes. Firstly, reporter genes were designed and constructed using PQS-encoding genes that appear naturally in the *P. falciparum* genome. The predominant gene group containing PQSs is the *var* virulence genes, but these are prohibitively large for cloning and many of the *var*-associated PQSs actually occur in the *var* upstream region rather than the coding sequence. Therefore, two genes from a second family of variantly-expressed virulence genes were chosen: the *rifin* genes *PF3D7_0700200* and *PF3D7_1254400*. Only three out of ~200 *rifin* genes encode PQSs, compared to a larger proportion (30 out of 63) of the *var* genes (5) but crucially *rifin*s have small sequences of ~1kb that are tractable for cloning. The complete ORFs of these genes were therefore cloned into expression vectors with C-terminal tags which allowed their transcripts to be distinguished from those of the many other highly-homologous *rifin* genes in the family. *PF3D7_0700200* encodes a PQS in the sense orientation and *PF3D7_1254400*, in the antisense orientation. The latter gene proved not to be expressed when transfected into parasites (a common issue with variantly-expressed gene families, data not shown) but the other gene, *PF3D7_0700200*, was successfully transcribed in transfected parasites.

To confirm that the PQS within this reporter gene could indeed form a G-quadruplex structure, ^{1}H NMR experiments were conducted with a synthetic oligonucleotide from this gene (Fig. 4A), revealing the presence of characteristic imino protons signals (chemical shift between 10 and 12 ppm) when the oligo was folded in the presence of potassium (Fig. 4B). The oligo also showed a 295 nm thermal denaturation curve typical of G-quadruplexes, with a half denaturation (T_m)

at 49°C (Fig. 4C), indicating that the G-quadruplex formed by this sequence is likely to be stable at physiological temperature.

To confirm that this G-quadruplex structure could be targeted by G-quadruplex-binding compounds, parasites carrying the construct were treated for 6 hours with 0.75μM TMPyP4 or TMPyP2 (approximately the 48-hour EC_{50} dose of TMPyP4). Because these compounds do not have any immediate cytocidal effect, the 6-hour exposure did not cause any visible change in parasite morphology but it clearly suppressed reporter gene expression relative to the expression of housekeeping genes. TMPyP4 – which is the more potent G-quadruplex-binding analog – had a much stronger effect on transcription than TMPyP2 (Fig. 4D). The same assay was then carried out with ~ 48-hour EC_{50} doses of quarfloxin and NMM, but owing to the rapid cytocidal effect previously established for these compounds, only one hour of exposure was used in an attempt to avoid non-specific results associated with parasite death. Reporter gene expression was markedly suppressed by both quarfloxin and NMM (Fig. 4E).

Having shown that quarfloxin, in common with other G-quadruplex-binding compounds, can indeed affect the expression of a PQS-encoding gene, we turned to the expression of rRNA genes, which was previously shown to be suppressed by quarfloxin in both human cells and trypanosomes (17, 18). *Plasmodium* does not encode its rRNA in conventional tandem arrays and possesses only a few rRNA genes scattered on various chromosomes (2)(Fig. 5A): these are expressed stage-specifically with A-type genes being used in the blood stages and S-type genes in mosquito stages (32). Therefore, RT-PCR was conducted for the A-type genes after 1 hour of quarfloxin exposure, as in Fig. 4E. In contrast to the effect seen in *T.*

brucei, in which rRNA precursor transcripts were dramatically suppressed after just 15 minutes of quarfloxin exposure (17), there was no loss of these transcripts in *P. falciparum*; in fact the transcript level rose somewhat (Fig. 5B) and this effect was broadly mirrored in the level of mature 18S rRNA (Fig. 5C). Thus, the mode of action of quarfloxin in *P. falciparum* is evidently different from that previously characterised in both *T. brucei* and human cells.

As a fluoroquinolone, quarfloxin shares limited structural similarity with the well-established 4-aminoquinoline drugs (chloroquine, mefloquine, etc.), which kill *Plasmodium* parasites by inhibiting haemozoin crystallisation in the food vacuole (33). This therefore presented another possible mode of action for quarfloxin, but the drug's high potency against pre-replicative ring stages, the fact that its BRRoK profile is distinct from that of chloroquine, and the fact that the drug does not prevent haem crystallisation *in vitro* (Fig. S5) all suggest that quarfloxin does not actually act in the same mode as 4-aminoquinolines. The true target of quarfloxin in *Plasmodium* parasites remains unknown, but it is apparently neither the haem detoxification pathway (Fig. S5) nor the production of ribosomal RNA (Fig. 5).

DISCUSSION

This is to our knowledge the first experimental investigation of the biological roles of G-quadruplex motifs in the malaria parasite *P. falciparum*. We demonstrate that G-quadruplex DNA can be detected in this parasite and that disrupting the normal processing of G-quadruplex motifs impairs parasite growth *in vitro*. It is important to note that sequences with the potential to form G-quadruplexes are very scarce in the *P. falciparum* genome and that the G-quadruplexes detected in *P. falciparum* nuclei using structure-specific antibodies are likely to be primarily in telomeres, since the

307 majority of all PQSs in *P. falciparum* are tandemly arrayed in telomere repeats (10)
308 and such antibodies probably cannot detect G-quadruplexes at single-motif
309 resolution (34). (Indeed, the G-quadruplex signal seen in late-stage parasites
310 appears to be strongest in nuclear-peripheral foci, as expected of telomeric DNA.)
311 However, it is also important to note that the G-quadruplex-forming potential of the *P.*
312 *falciparum* genome may be underestimated by standard *in silico* algorithms, as was
313 recently demonstrated by sequencing the human genome with a G-quadruplex-
314 sensitive method (8): this empirical approach detected many more G-quadruplexes
315 than the *in silico* method of scanning the genome for repetitions of G_3N_{1-7} (7). For
316 the *P. falciparum* genome, a relatively relaxed predictive algorithm was used in our
317 previous study (G_3N_{0-11}) and this still found just 80 non-telomeric PQSs (5); however,
318 the algorithm will overlook many of the non-canonical G-quadruplexes detected in
319 the human genome, such as 'bulged' G-quadruplexes (8) and inter-strand rather
320 than intra-strand G-quadruplexes (9). Finally, the structure-specific antibody used
321 here detects only DNA and not RNA G-quadruplexes, so the existence of RNA G-
322 quadruplexes in *P. falciparum* remains to be confirmed.

323 Several G-quadruplex-stabilising compounds were shown to inhibit malaria
324 parasite growth, including the Phase-2 anticancer drug quarfloxin, which was potent
325 and relatively fast-acting against both ring and trophozoite parasites. An ideal
326 antimalarial should kill parasites at all stages of the intraerythrocytic cycle (and,
327 indeed, ideally at non-erythrocytic phases of the lifecycle as well). For example, the
328 current first-line antimalarial drug, artemisinin, kills prereplicative ring stages as well
329 as trophozoites and schizonts, whereas older antimalarials such as chloroquine and
330 antifolates are highly active only against replicative stages. Whilst it is not essential
331 to elucidate the molecular mechanism(s) of an antiplasmodial compound prior to

clinical development – indeed, the mechanism of artemisinin remains poorly understood – this information can help in predicting the development of drug resistance and cross-resistance. Therefore, we investigated the mode of action for quarfloxin. We found no evidence that quarfloxin kills parasites by inducing telomere dysfunction, despite the predominance of PQSs in telomere repeats, since telomere maintenance appeared to be normal after up to 15 cycles of growth in quarfloxin. This does not conclusively exclude the possibility of an acutely lethal telomere dysfunction being induced at higher drug exposures, but the tools to assess this in *P. falciparum* are lacking: the parasite lacks the variant histone γH2AX (35) which is commonly used to detect DNA damage foci, and also lacks all components of the conventional telomere shelterin complex (36).

In the absence of any clear effect on telomeres, we assessed the possibility that quarfloxin might kill parasites by preventing the proper expression of G-quadruplex-containing genes. 41 PQSs are predicted in non-*var* genes (5), many of which may be essential (by contrast, *var* gene expression is dispensable *in vitro* (37), albeit vital *in vivo* for virulence phenotypes such as intravascular adhesion, antigenic variation and immune evasion). As proof of concept, a G-quadruplex-encoding rifin reporter gene was cloned, validated and transfected into parasites, and its expression was shown to be suppressed by all of the G-quadruplex-binding compounds tested. This is the first demonstration of G-quadruplex-dependent gene expression in *P. falciparum* and it conforms to a model in which sense-strand G-quadruplexes, when stably formed in DNA, can inhibit transcription by RNA polymerase II.

We then assessed the model for quarfloxin action that was previously reported in trypanosomes and human cells: suppression of rRNA transcription by RNA polymerase I (17, 18). We focussed only upon the nuclear rRNA genes, not those encoded in the apicoplast organelle, because interfering with protein synthesis in the apicoplast of *P. falciparum* gives a characteristic 'delayed death' phenotype, with death occurring only in the second growth cycle after drug addition (38), whereas the parasite death observed here with quarfloxin was very rapid, making apicoplast ribosomes highly unlikely to be a key target.

Although *P. falciparum* expresses its rRNA genes via RNA polymerase I, it does not maintain these genes in conventional tandem arrays (2) and furthermore, most of the parasite's rRNA genes are not predicted to contain PQSs (5). Only one atypical locus on chromosome 8, *PF3D7_0830000*, which contains 5.8S and 28S rRNA genes but no 18S rRNA, contains a $G_3N_{0\text{-}11}$ motif. It is therefore arguably not surprising that we did not find any evidence for acute suppression of rRNA transcription by quarfloxin. Instead, other essential gene(s) that encode PQSs may be targeted by quarfloxin, and other G-quadruplex-related modes of action such as acute induction of DNA damage or telomere dysfunction cannot yet be ruled out. (It also remains possible that G-quadruplexes are simply not involved: we are currently conducting further work to establish quarfloxin's actual mode of action in *P. falciparum*, having established that at least one other predictable possibility – the inhibition of haemozoin crystallisation – is not consistent with our data.) More generally, the very diverse rates of kill for the different compounds tested here suggest that they may vary not only in their absolute affinity for G-quadruplexes but also in the subset of G-quadruplexes that each compound targets within the genome.

In conclusion, this work shows that G-quadruplex-binding compounds may have the potential to be repositioned as antimalarials. Quarfloxin is potent and fast-acting (at least *in vitro*), it has well-characterised pharmacodynamics in humans as established from previous cancer trials, and the selective window is at least 40x on *P. falciparum* over human cells (111nM compared to 4.44μM on human breast epithelial cells, as reported by Kerry *et al.* (17)). G-quadruplex biology in malaria parasites thus constitutes an exciting area for future study, both to improve our understanding of basic biology and virulence gene control in this parasite, and also to support the discovery of novel targets for antimalarial drug development.

MATERIALS AND METHODS

Parasite culture and drugs

The 3D7 strain of *P. falciparum* was obtained from the Malaria Research and Reference Reagent Resource Center (MR4) and the NF54^{attB} strain, from Professor David Fidock. The luciferase-expressing Dd2 strain is previously described (39). Parasites were cultured as previously described (40). Parasite growth and morphology was assessed on blood smears stained with Hemacolor (Merck). Synchronised parasite cultures were obtained by performing two treatments with 5 % D-sorbitol (41) 42 h apart, to yield an approximately 4-h window of ring stage parasites. 3D7 parasites were used in all experiments except the gene-expression studies, which were performed in NF54^{attB}, and the BRRoK assays which were performed in both NF54 and Dd2 backgrounds. The compounds NMM, TMPyP4 and TMPyP2 were obtained from Frontier Scientific and quarfloxin from Tetragene LLC, solubilized in water and stored without exposure to light at -20°C.

Immunofluorescence assay

For G-quadruplex detection using the IH6 antibody, air-dried blood smears were fixed with 2% paraformaldehyde/PBS for 2 min and then 90% acetone/10% methanol for 2 min at 4°C. Smears were air-dried, blocked with 1% BSA/PBS and sequentially treated with primary and secondary antibodies. Antibodies used were the anti-G-quadruplex monoclonal IH6 (Biorbyt), rabbit polyclonal antibodies to the *P. falciparum* cis-Golgi marker ERD2 (obtained from MR4, MRA-1 (42)), Cy3-conjugated anti-rabbit IgG (Jackson ImmunoResearch) and Alexa Fluor 488-conjugated anti-mouse IgG (Thermo Fisher Scientific). For enzymatic treatments, slides were incubated after fixation with 0.12 U μL^{-1} Turbo DNase (Albion) or with 100 µg mL^{-1} RNase A (Thermo Fischer Scientific) for 1 h at 37 °C. Slides were mounted with ProLong Diamond containing DAPI (Thermo Fisher Scientific) and were imaged with an EVOS cell imaging system (Thermo Fisher Scientific). Parasites were visualised and images captured using the same exposure for each fluorochrome across all treatments.

For G-quadruplex detection using the BG4 antibody, parasites were first removed from host erythrocytes using 0.4% saponin, then fixed in 4% paraformaldehyde/PBS. Fixed parasites were dispensed onto a 12 multi-spot well slide (Thermo Fisher Scientific) and air-dried. All subsequent steps were carried out at room temperature in 10µL volume. The parasites were permeabilized with 0.1% Triton in PBS, washed with PBS, then blocked in 3% bovine serum albumin in PBS for 1.5 h. Antibody staining steps were: flag-tagged BG4 antibody (EMD Millipore) for 1.5h; rabbit anti-flag antibody (Cell Signalling Technology) for 1.5h; Cy3 conjugated-anti rabbit secondary antibody (Jackson ImmunoResearch) for 1h. Slides were washed three times with PBS after each step. Mounting and visualisation were as described above.

Malaria SYBR Green I-based fluorescence (MSF) assay

MSF assays were carried out as previously described (26). Trophozoite-stage cultures (75 µL, 1 % parasitaemia, 4 % haematocrit) were added to 96-multiwell plates containing triplicate wells of 75 µL complete medium pre-dosed with compounds. On each assay plate, 3 wells containing 150 µL trophozoite-stage culture (0.5 % parasitaemia, 2 % haematocrit) in the absence of drugs served as a positive control (100% growth). The outer wells of each 96-well plate were filled with 200 µL of medium to prevent evaporation. Plates were incubated for 48 h in a gassed (1% O_2, 3% CO_2, and 96% N_2) chamber at 37 °C. Following this, 100 µL of the sample from each well was mixed with 100 µL MSF lysis buffer (20 mM Tris pH 7.5, 5 mM EDTA, 0.008% saponin, 0.8% Triton X-100) supplemented with 0.2 µL mL^{-1} of SYBR Green I (Sigma). After a 1-h incubation in the dark at room temperature, SYBR Green I fluorescence was measured using the blue fluorescent module (excitation 490 nm: emission 510-570 nm) of a GloMax multidetection system (Promega). Percentage parasite growth was calculated as follows: $100x[\mu_{(s)} - \mu_{(-)}/\mu_{(+)} - \mu_{(-)}]$ where $\mu_{(s)}$, $\mu_{(-)}$ and $\mu_{(+)}$ are the means of the fluorescent readouts from sample wells, from control wells without drug (100 % growth) and from wells with the maximum drug concentration (0 % growth), respectively. EC_{50} values were determined by plotting log concentration normalized response curves using GraphPad Prism v5.0 (GraphPad Software, Inc., San Diego, CA) from the mean of three independent biological repeats.

Bioluminescence Relative Rate of Kill (BRRoK) assay

BRRoK assays were carried out as described (31). Trophozoite- cultures of Dd2^{luc} or NF54^{luc} (100µl, 2% parasitaemia, 4% haematocrit) were added to 96-multiwell

plates containing 100µl of pre-dosed complete culture medium (three-fold EC_{50} dilution series, 9xEC_{50} to 0.33xEC_{50} for each compound tested), mixed by pipetting and incubated for 6 h at 37°C. Samples of 40 µL were removed from each well and the bioluminescence signal was measured using the luciferase single-step lysis protocol (43). Controls in each biological replicate consisted of trophozoite stage culture with no drug added (100% bioluminescence). The normalised bioluminescence data from three biological repeats was plotted as a proportion of the untreated control, with reference data for benchmark antimalarial compounds sourced from (31).

Flow Cytometry

Parasite cultures were washed in PBS and then stained for flow cytometry using SYBR Green 1 diluted 1:2000 in PBS, incubated at room temperature without light exposure for 20 minutes. Parasites were then fixed in 4% formalin (Sigma) in PBS, incubated at 4°C for 15 minutes, before thorough washing in PBS and analysis using forward scatter and the green fluorescence channel of a Guava easyCyte System (Merck Millipore).

Southern blotting

Genomic DNA was extracted from parasites using the QIAamp DNA Blood Mini Kit (Qiagen) and digested with restriction enzymes *Alu*I, *Dde*I, *Mbo*II and *Rsa*I as previously described (44). Digested genomic DNA was resolved on a 1 % agarose gel, transferred to GenScreen Plus (PerkinElmer) and hybridised with a probe specific for telomeres (45), labelled with alkaline phosphatase (AlkPhos Direct Labelling and Detection system, GE Healthcare) and then imaged according to the kit manufacturer's directions.

Plasmid construction and parasite transfection to generate Rifin-GFP reporter line

To generate the G-quadruplex reporter line the *rifin* gene *PF3D7_0700200* was amplified using the primers TGCCTAGGATGAAAATCCATTATATTAAT and ACCGTACGTTCTTTTAATAGTTTTATGTATG, then cloned upstream of the C-terminal GFP tag in the pLN-ENR-GFP plasmid (46) to generate the plasmid pLN-Rif0700200-GFP. NF54^{attB} parasites were transfected with pLN-Rif0700200-GFP and maintained on BSD selection as previously described (46, 47).

Biophysical characterization of G-quadruplex formation

Oligonucleotide TTTGGGAGGGCTTGTTCCGGGAATGGGTT was purchased from Eurofins Genomics (Ebersberg, Germany) and was resuspended in MilliQ water to generate a stock solution at 400 µM. Before experiments, the oligonucleotide was annealed by heating at 90 °C for 3 minutes. Cation solution (KCl or LiCl) and lithium cacodylate were then added to reach final concentrations of 150 and 10 mM respectively, and a pH of 7.4. For thermal denaturation, oligonucleotide final concentration was 2.5 µM and UV absorption was recorded at 295 nm on a Uvikon XS spectrophotometer (Seconam), using 1 cm path-length quartz cell (Hellma, type No. 115B-QS, France). NMR samples were prepared by dissolving the oligonucleotides in H_2O/D_2O 95/5, lithium cacodylate 10 mM, pH 7.4 for a final oligonucleotide concentration of 200 µM. NMR data were collected at 500 MHz on a Bruker Avance spectrometer (fitted with a TCI triple resonance cryo-probe with z-axis gradient). 1D ^{1}H spectra were recorded at a temperature of 25°C. Water suppression was achieved using excitation sculpting with gradients (48).

Gene expression analysis

Total RNA was extracted from mixed-stage cultures of parasites transfected with pLN-Rif0700200-GFP using the RNeasy kit (Qiagen). Extracted RNA was treated with DNaseI and cDNA was subsequently synthesised using the iScript cDNA Synthesis Kit (BIO-RAD). cDNA was checked for genomic DNA contamination by PCR across the intron of the gene PF3D7_0424300, as previously described (49). Relative gene expression was determined by real-time PCR using a StepOnePlus Real-Time PCR machine (ThermoFisher Scientific) and the SensiFAST SYBR Hi-ROX kit (Bioline) on synthesised cDNAs. Cycling conditions were 95°C for 3 minutes, 40 cycles of 95°C for 15 seconds, 45°C for 40 seconds, 60°C for 1 minute. The three housekeeping genes used as controls were PF3D7_0717700 (seryl-tRNA synthetase), PF3D7_1444800 (fructose bisphosphate aldolase) and PF3D7_1246200 (actin): primers for these genes are previously described (50). A1 and A2 rRNA transcripts, and mature 18S rRNA, were also measured using primers previously described (51). The GFP-tagged reporter gene was measured using the GFP-specific primers GATGGAAGCGTTCAACTAGCAGACC and AGCTGTTACAAACTCAAGAAGGACC. $\Delta\Delta$Ct analysis (Ct, threshold cycle) was used to calculate the relative copy number of each target gene relative to the average Ct of the three control genes. All experiments were conducted in both biological and technical duplicate.

Haem crystallisation assay

This assay was carried out as previously described (52), with the slight modification of using NP-40 rather than Tween-20 to initiate crystallisation (as per (53)). 500μM quarfloxin was added because previous work showed that the equivalent level of chloroquine could produce the maximal (75%) inhibition of crystallisation (52). The conventional readout of this assay, haem absorbance at 415nm, was precluded by

interference from the strong intrinsic colour of quarfloxin, and the assay could therefore be assessed only by non-quantitative visual observation of the crystals formed.

AUTHOR CONTRIBUTIONS

LMH, KRM and FN conducted and designed experiments, analysed data and produced figures; MTF conducted BRRoK assays, NS and CD performed biophysical characterisation of G-quadruplex DNA; PD designed the BRRoK assays, analysed data and edited the manuscript; CJM designed the study, conducted experiments, analysed data and wrote the manuscript. All authors read and approved the final manuscript.

FUNDING INFORMATION

UK Medical Research Council (grants MR/K000535/1 and MR/L008823/1) to CJM, Jean Shanks Foundation grant to KRM, PhD studentship from the Nigerian Tertiary Education TrustFund to MTF.

The funders had no role in study design, data collection and interpretation, or the decision to submit the work for publication

ACKNOWLEDGEMENTS

We are grateful to Tetragene LLC for supplying quarfloxin, to Dr. Pascal De Tullio (ULg) for help with NMR experiments, and to Adriana Adolfi and Rinal Sahputra for conducting preliminary work in the lab on G-quadruplex-stabilising drugs in *P. falciparum*.

REFERENCES

1. **WHO.** 2016. World Malaria Report 2016. WHO website doi:http://www.who.int/malaria/publications/world_malaria_report/en/.
2. **Gardner MJ, Hall N, Fung E, White O, Berriman M, Hyman RW, Carlton JM, Pain A, Nelson KE, Bowman S, Paulsen IT, James K, Eisen JA, Rutherford K, Salzberg SL, Craig A, Kyes S, Chan MS, Nene V, Shallom SJ, Suh B, Peterson J, Angiuoli S, Pertea M, Allen J, Selengut J, Haft D, Mather MW, Vaidya AB, Martin DM, Fairlamb AH, Fraunholz MJ, Roos DS, Ralph SA, McFadden GI, Cummings LM, Subramanian GM, Mungall C, Venter JC, Carucci DJ, Hoffman SL, Newbold C, Davis RW, Fraser CM, Barrell B.** 2002. Genome sequence of the human malaria parasite Plasmodium falciparum. Nature **419:**498-511.
3. **Carlton JM, Adams JH, Silva JC, Bidwell SL, Lorenzi H, Caler E, Crabtree J, Angiuoli SV, Merino EF, Amedeo P, Cheng Q, Coulson RM, Crabb BS, Del Portillo HA, Essien K, Feldblyum TV, Fernandez-Becerra C, Gilson PR, Gueye AH, Guo X, Kang'a S, Kooij TW, Korsinczky M, Meyer EV, Nene V, Paulsen I, White O, Ralph SA, Ren Q, Sargeant TJ, Salzberg SL, Stoeckert CJ, Sullivan SA, Yamamoto MM, Hoffman SL, Wortman JR, Gardner MJ, Galinski MR, Barnwell JW, Fraser-Liggett CM.** 2008. Comparative genomics of the neglected human malaria parasite Plasmodium vivax. Nature **455:**757-763.
4. **Otto TD, Bohme U, Jackson AP, Hunt M, Franke-Fayard B, Hoeijmakers WA, Religa AA, Robertson L, Sanders M, Ogun SA, Cunningham D, Erhart A, Billker O, Khan SM, Stunnenberg HG, Langhorne J, Holder AA, Waters AP, Newbold CI, Pain A, Berriman M, Janse CJ.** 2014. A comprehensive evaluation of rodent malaria parasite genomes and gene expression. BMC Biol **12:**86.
5. **Stanton A, Harris LM, Graham G, Merrick CJ.** 2016. Recombination events among virulence genes in malaria parasites are associated with G-quadruplex-forming DNA motifs. BMC Genomics **17:**859.
6. **Gilbert DE, Feigon J.** 1999. Multistranded DNA structures. Curr Opin Struct Biol **9:**305-314.
7. **Huppert JL, Balasubramanian S.** 2005. Prevalence of quadruplexes in the human genome. Nucleic Acids Res **33:**2908-2916.
8. **Chambers VS, Marsico G, Boutell JM, Di Antonio M, Smith GP, Balasubramanian S.** 2015. High-throughput sequencing of DNA G-quadruplex structures in the human genome. Nat Biotechnol **33:**877-881.
9. **Kudlicki AS.** 2016. G-Quadruplexes Involving Both Strands of Genomic DNA Are Highly Abundant and Colocalize with Functional Sites in the Human Genome. PLoS One **11:**e0146174.
10. **Smargiasso N, Gabelica V, Damblon C, Rosu F, De Pauw E, Teulade-Fichou MP, Rowe JA, Claessens A.** 2009. Putative DNA G-quadruplex formation within the promoters of Plasmodium falciparum var genes. BMC Genomics **10:**362.
11. **De Cian A, Grellier P, Mouray E, Depoix D, Bertrand H, Monchaud D, Teulade-Fichou MP, Mergny JL, Alberti P.** 2008. Plasmodium telomeric sequences: structure, stability and quadruplex targeting by small compounds. Chembiochem **9:**2730-2739.
12. **Calvo EP, Wasserman M.** 2016. G-Quadruplex ligands: Potent inhibitors of telomerase activity and cell proliferation in Plasmodium falciparum. Mol Biochem Parasitol **207:**33-38.
13. **Paeschke K, Simonsson T, Postberg J, Rhodes D, Lipps HJ.** 2005. Telomere end-binding proteins control the formation of G-quadruplex DNA structures in vivo. Nature Structural and Molecular Biology **12:**847-854.
14. **Siddiqui-Jain A, Grand CL, Bearss DJ, Hurley LH.** 2002. Direct evidence for a G-quadruplex in a promoter region and its targeting with a small molecule to repress c-MYC transcription. Proc Natl Acad Sci U S A **99:**11593-11598.

15. **Kruisselbrink E, Guryev V, Brouwer K, Pontier DB, Cuppen E, Tijsterman M.** 2008. Mutagenic capacity of endogenous G4 DNA underlies genome instability in FANCJ-defective C. elegans. Current Biology **18:**900-905.
16. **Koole W, van Schendel R, Karambelas AE, van Heteren JT, Okihara KL, Tijsterman M.** 2014. A Polymerase Theta-dependent repair pathway suppresses extensive genomic instability at endogenous G4 DNA sites. Nat Commun **5:**3216.
17. **Kerry LE, Pegg EE, Cameron DP, Budzak J, Poortinga G, Hannan KM, Hannan RD, Rudenko G.** 2017. Selective inhibition of RNA polymerase I transcription as a potential approach to treat African trypanosomiasis. PLoS Negl Trop Dis **11:**e0005432.
18. **Drygin D, Siddiqui-Jain A, O'Brien S, Schwaebe M, Lin A, Bliesath J, Ho CB, Proffitt C, Trent K, Whitten JP, Lim JK, Von Hoff D, Anderes K, Rice WG.** 2009. Anticancer activity of CX-3543: a direct inhibitor of rRNA biogenesis. Cancer Res **69:**7653-7661.
19. **Balasubramanian S, Hurley LH, Neidle S.** 2011. Targeting G-quadruplexes in gene promoters: a novel anticancer strategy? Nat Rev Drug Discov **10:**261-275.
20. **Drygin D, Rice WG, Grummt I.** 2010. The RNA polymerase I transcription machinery: an emerging target for the treatment of cancer. Annu Rev Pharmacol Toxicol **50:**131-156.
21. **Papadopoulos K, Mita A, Ricart A, Hufnagel D, Northfelt D, Von Hoff D, Darjania L, Lim J, Padgett C, Marschke R.** 2007. Pharmacokinetic findings from the phase I study of Quarfloxin (CX-3543): a protein-rDNA quadruplex inhibitor, in patients with advanced solid tumors. Molecular Cancer Therapeutics **6**.
22. **Biffi G, Di Antonio M, Tannahill D, Balasubramanian S.** 2014. Visualization and selective chemical targeting of RNA G-quadruplex structures in the cytoplasm of human cells. Nat Chem **6:**75-80.
23. **Biffi G, Tannahill D, McCafferty J, Balasubramanian S.** 2013. Quantitative visualization of DNA G-quadruplex structures in human cells. Nat Chem **5:**182-186.
24. **Henderson A, Wu Y, Huang YC, Chavez EA, Platt J, Johnson FB, Brosh RM, Jr., Sen D, Lansdorp PM.** 2014. Detection of G-quadruplex DNA in mammalian cells. Nucleic Acids Res **42:**860-869.
25. **Schaffitzel C, Berger I, Postberg J, Hanes J, Lipps HJ, Pluckthun A.** 2001. In vitro generated antibodies specific for telomeric guanine-quadruplex DNA react with Stylonychia lemnae macronuclei. Proc Natl Acad Sci U S A **98:**8572-8577.
26. **Smilkstein M, Sriwilaijaroen N, Kelly JX, Wilairat P, Riscoe M.** 2004. Simple and inexpensive fluorescence-based technique for high-throughput antimalarial drug screening. Antimicrob Agents Chemother **48:**1803-1806.
27. **Arthanari H, Basu S, Kawano TL, Bolton PH.** 1998. Fluorescent dyes specific for quadruplex DNA. Nucleic Acids Res **26:**3724-3728.
28. **De Matteis F, Gibbs AH, Smith AG.** 1980. Inhibition of protohaem ferro-lyase by N-substituted porphyrins. Structural requirements for the inhibitory effect. Biochem J **189:**645-648.
29. **Izbicka E, Wheelhouse RT, Raymond E, Davidson KK, Lawrence RA, Sun D, Windle BE, Hurley LH, Von Hoff DD.** 1999. Effects of cationic porphyrins as G-quadruplex interactive agents in human tumor cells. Cancer Res **59:**639-644.
30. **Han FX, Wheelhouse RT, Hurley LH.** 1999. Interactions of TMPyP4 and TMPyP2 with Quadruplex DNA. Structural Basis for the Differential Effects on Telomerase Inhibition. Journal of the American Chemical Society doi:10.1021/ja984153m**:**10.
31. **Ullah I, Sharma R, Biagini GA, Horrocks P.** 2017. A validated bioluminescence-based assay for the rapid determination of the initial rate of kill for discovery antimalarials. J Antimicrob Chemother **72:**717-726.
32. **Waters AP, Syin C, McCutchan TF.** 1989. Developmental regulation of stage-specific ribosome populations in Plasmodium. Nature **342:**438-440.

33. **Slater AF.** 1993. Chloroquine: mechanism of drug action and resistance in Plasmodium falciparum. Pharmacol Ther **57:**203-235.
34. **Kwok CK, Merrick CJ.** 2017. G-Quadruplexes: Prediction, Characterization, and Biological Application. Trends Biotechnol doi:10.1016/j.tibtech.2017.06.012.
35. **Miao J, Fan Q, Cui L, Li J, Li J, Cui L.** 2006. The malaria parasite Plasmodium falciparum histones: organization, expression, and acetylation. Gene **369:**53-65.
36. **Bertschi NL, Toenhake CG, Zou A, Niederwieser I, Henderson R, Moes S, Jenoe P, Parkinson J, Bartfai R, Voss TS.** 2017. Malaria parasites possess a telomere repeat-binding protein that shares ancestry with transcription factor IIIA. Nat Microbiol **2:**17033.
37. **Dzikowski R, Deitsch KW.** 2008. Active transcription is required for maintenance of epigenetic memory in the malaria parasite Plasmodium falciparum. J Mol Biol **382:**288-297.
38. **Dahl EL, Rosenthal PJ.** 2007. Multiple antibiotics exert delayed effects against the Plasmodium falciparum apicoplast. Antimicrob Agents Chemother **51:**3485-3490.
39. **Wong EH, Hasenkamp S, Horrocks P.** 2011. Analysis of the molecular mechanisms governing the stage-specific expression of a prototypical housekeeping gene during intraerythrocytic development of P. falciparum. J Mol Biol **408:**205-221.
40. **Trager W, Jensen JB.** 1976. Human malaria parasites in continuous culture. Science **193:**673-675.
41. **Lambros C, Vanderberg JP.** 1979. Synchronization of Plasmodium falciparum erythrocytic stages in culture. J Parasitol **65:**418-420.
42. **Elmendorf HG, Haldar K.** 1993. Identification and localization of ERD2 in the malaria parasite Plasmodium falciparum: separation from sites of sphingomyelin synthesis and implications for organization of the Golgi. EMBO J **12:**4763-4773.
43. **Hasenkamp S, Wong EH, Horrocks P.** 2012. An improved single-step lysis protocol to measure luciferase bioluminescence in Plasmodium falciparum. Malar J **11:**42.
44. **Figueiredo LM, Freitas-Junior LH, Bottius E, Olivo-Marin JC, Scherf A.** 2002. A central role for Plasmodium falciparum subtelomeric regions in spatial positioning and telomere length regulation. Embo J **21:**815-824.
45. **Bottius E, Bakhsis N, Scherf A.** 1998. Plasmodium falciparum telomerase: de novo telomere addition to telomeric and nontelomeric sequences and role in chromosome healing. Mol Cell Biol **18:**919-925.
46. **Adjalley SH, Lee MC, Fidock DA.** 2010. A method for rapid genetic integration into Plasmodium falciparum utilizing mycobacteriophage Bxb1 integrase. Methods Mol Biol **634:**87-100.
47. **Adjalley SH, Johnston GL, Li T, Eastman RT, Ekland EH, Eappen AG, Richman A, Sim BK, Lee MC, Hoffman SL, Fidock DA.** 2011. Quantitative assessment of Plasmodium falciparum sexual development reveals potent transmission-blocking activity by methylene blue. Proc Natl Acad Sci U S A **108:**E1214-1223.
48. **Hwang TL, Shaka, A. J. .** 1995. Water Suppression That Works. Excitation Sculpting using Arbitary Waveforms and Pulsed Field Gradients. Journal of Magnetic Resonance **Series A**.
49. **Frank M, Dzikowski R, Amulic B, Deitsch K.** 2007. Variable switching rates of malaria virulence genes are associated with chromosomal position. Mol Microbiol **64:**1486-1498.
50. **Dzikowski R, Frank M, Deitsch K.** 2006. Mutually exclusive expression of virulence genes by malaria parasites is regulated independently of antigen production. PLoS Pathog **2:**e22.
51. **Mancio-Silva L, Lopez-Rubio JJ, Claes A, Scherf A.** 2013. Sir2a regulates rDNA transcription and multiplication rate in the human malaria parasite Plasmodium falciparum. Nat Commun **4:**1530.
52. **Huy NT, Uyen DT, Maeda A, Trang DT, Oida T, Harada S, Kamei K.** 2007. Simple colorimetric inhibition assay of heme crystallization for high-throughput screening of antimalarial compounds. Antimicrob Agents Chemother **51:**350-353.

53. **Sandlin RD, Carter MD, Lee PJ, Auschwitz JM, Leed SE, Johnson JD, Wright DW.** 2011. Use of the NP-40 detergent-mediated assay in discovery of inhibitors of beta-hematin crystallization. Antimicrob Agents Chemother **55:**3363-3369.

FIGURE LEGENDS

Figure 1: ***G-quadruplexes can be detected in P. falciparum parasites***

(A) Schematic of a G-quadruplex DNA motif. Guanine tetrads are shown as green squares and guanine backbones as dashed black lines. G-quartets stack on top of one another to form the quadruplex, which is stabilized by cations such as potassium (K+). An example of a PQS that could fold into such a structure is shown below.

(B) Immunofluorescence images showing G-quadruplexes detected with the structure-specific antibody IH6 in *P. falciparum* intraerythrocytic stages (3D7 parasite strain). Images are representative of 3 independent experiments, examining mixed-stage cultures.

(C) DNase treatment abolishes G-quadruplex (IH6) staining but has no effect on the distribution of a protein, ERD2, used as a control (middle row). RNase treatment has no discernible effect on G-quadruplex (IH6) staining (bottom row). Images are representative of 3 independent experiments.

Figure 2: ***G-quadruplex-binding drugs inhibit parasite growth***

(A) The G-quadruplex-binding drugs NMM, Quarfloxin, TMPyP2 and TmPyP4 inhibit the *in vitro* growth of *P. falciparum* (3D7 parasite strain) to varying extents. Percentage parasite growth is plotted as a function of [compound], error bars are standard error of the mean. The mean EC_{50} values from 3 independent Malaria SYBR Green I-based fluorescence (MSF) assays are tabulated and 95% confidence intervals are shown.

(B,C) EC_{50} concentration-dependent loss of normalised bioluminescence signal in BRRoK assays against (C) benchmark antimalarials and (D) G-quadruplex-stabilising compounds. The mean bioluminescence signal (normalised against an untreated control) remaining in $Dd2^{luc}$ *P. falciparum* after a 6 h exposure to the indicated fold-EC_{50} concentration of each drug or compound is plotted. Error bars represent ±SD from three biological replicates. ATQ, atovaquone; CQ, chloroquine; DHA, dihydroartemisinin; MQ, mefloquine; NMM, N-methyl-mesoporphyrin IX; QF, quarfloxin; TmPyP2, 5,10,15,20-tetra-(N-methyl-2-pyridyl) porphine; TmPyP4, 5,10,15,20-tetra-(N-methyl-4-pyridyl) porphine.

Figure 3: ***Quarfloxin kills ring-stage parasites as well as replicative stages***

Developmental stages of 3D7 parasites were assessed visually at 8 h intervals over a single growth cycle, starting at the mid-ring stage, either in the absence of drug or with quarfloxin added at 210nM (approximately 2x EC_{50}) at ring, trophozoite or schizont stages. Parasites were also analysed at 8 h intervals for DNA content by flow cytometry under each of these conditions. For morphology assessment, 50 parasites were counted at each timepoint and photographs show representative parasite morphology for each stage; dead parasites stained as a dense intracellular dot without clear morphological features. For flow cytometry, 200,000 parasites were counted in each sample.

Figure 4: ***G-quadruplex-binding drugs affect the expression of a G-quadruplex reporter gene***

(A) Oligonucleotide sequence from gene *PF3D7_0700200*, used in biophysical assays to confirm the folding of a G-quadruplex structure.

(B) ^{1}H NMR spectra, acquired at 37°C in 150 mM Li^{+} (top) and 150 mM K^{+} (bottom). Imino protons peaks are only present in K^{+}, in agreement with the inability of Li^{+} to stabilize G-quadruplex structures. The relatively low intensity of imino peaks in the K^{+} condition seems to indicate the presence of a floppy structure, potentially the consequence of the second long loop.

(C) Stability of the G-quadruplex as evaluated by thermal denaturation, followed at 295 nm.

(D) Expression of the GFP-tagged G-quadruplex reporter gene *PF3D7_0700200* in transgenic parasite cultures treated with 0.75μM TMPyP4 or TMPyP2 for 6 h. Expression was determined by quantitative real-time PCR using primer pair *GFP_F/R* as compared to average expression of three housekeeping genes encoding actin, seryl tRNA synthetase and fructose bisphosphate aldolase. The experiment was carried out in both biological and technical duplicate, error bars are standard error of the mean and statistical significance was assessed by 1-tailed t-test (**, $p<0.01$; ***, $p<0.001$).

(E) Expression of the GFP-tagged G-quadruplex reporter gene *PF3D7_0700200* in transgenic parasite cultures treated with 120nM quarfloxin or 80μM NMM for 1 h, determined as in (D).

Figure 5: ***Quarfloxin does not inhibit the expression of rRNA genes***

(A) **S**chematic showing the locations of rRNA-encoding units on the 14 chromosomes of the *P. falciparum* genome, together with their type (A, blood-stage expressed; S, mosquito-stage expressed). The locations of primers used to measure rRNA transcription are also shown**.**

(B) Expression of rRNA A1/2 transcripts in the same parasites as used in Figure 4E, after treatment with 120nM quarfloxin for 1 h. Target gene expression was determined relative to three control genes, as in Figure 4: error bars are standard error of the mean and statistical significance was assessed by 1-tailed t-test (**, $p<0.01$).

(C) Expression of mature 18S rRNA in the same parasites as used in Figure 4E, after treatment with 120nM quarfloxin for 1 h.

A

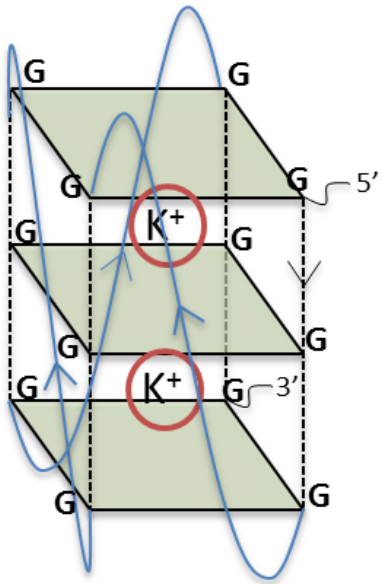

GGGAAGGGATGGGCAGGG

B

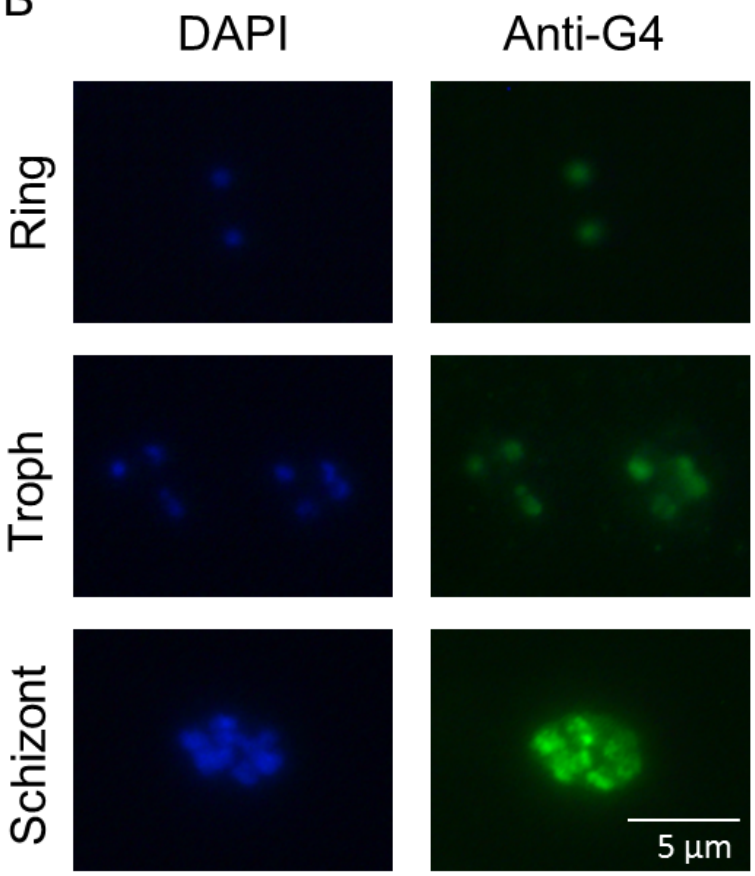

C

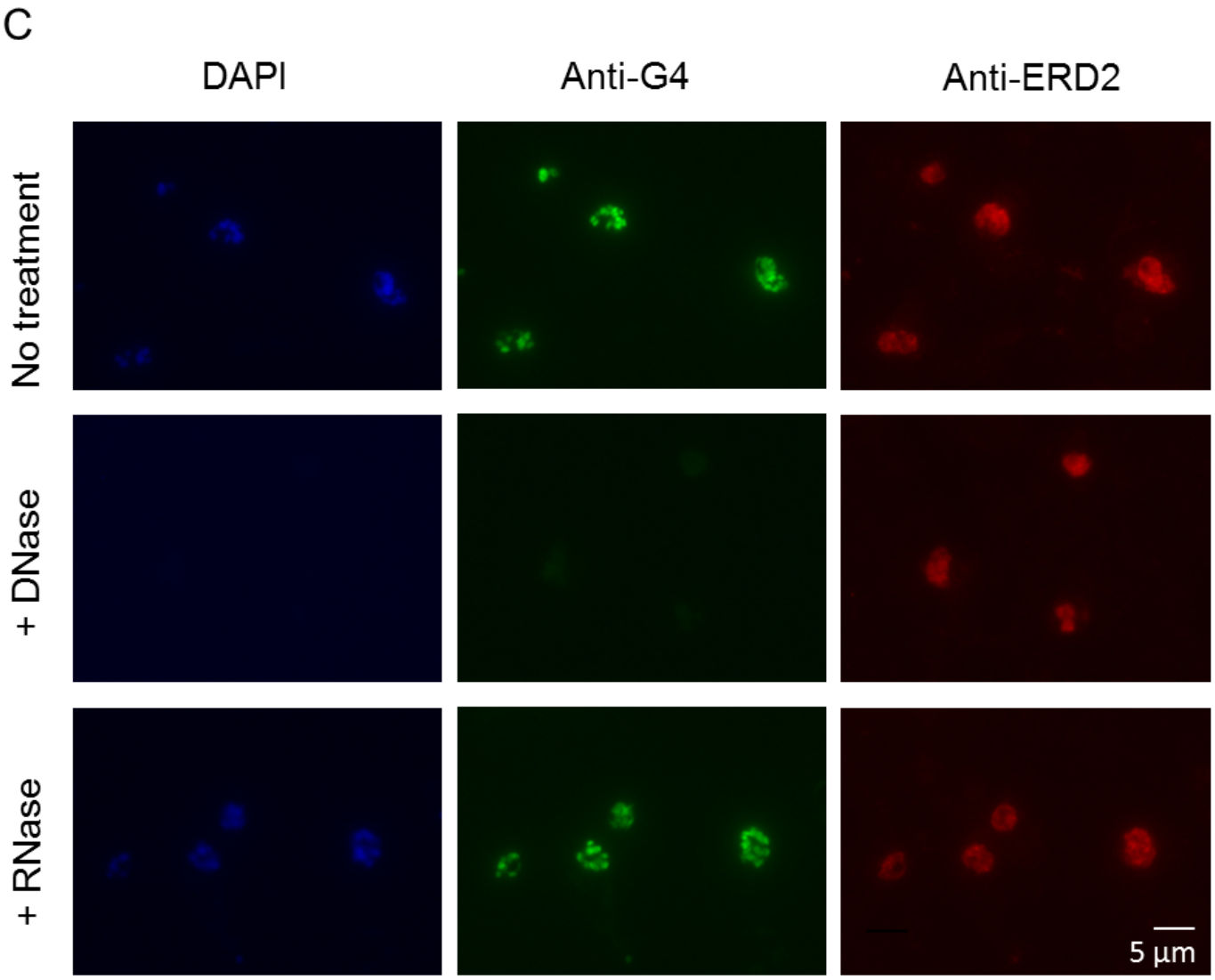

A

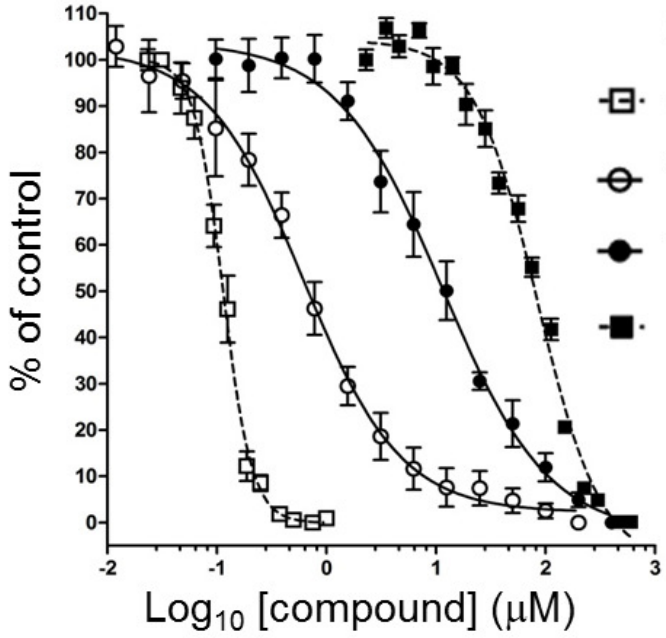

Compound	EC_{50} (μM)	95% C.I.
QF	0.11	0.108-0.120
TMPyP4	0.62	0.530-0.721
TMPyP2	11.4	8.79-14.9
NMM	84.7	70.1-101.2

B

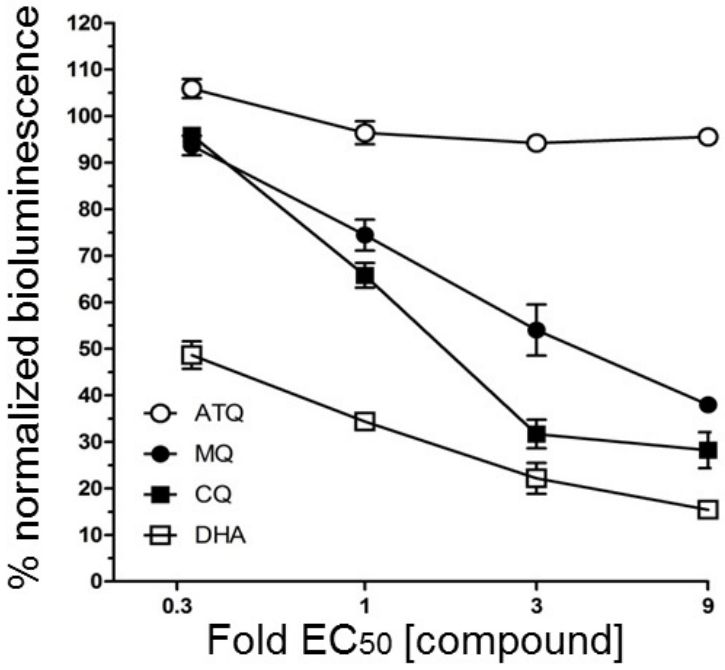

C

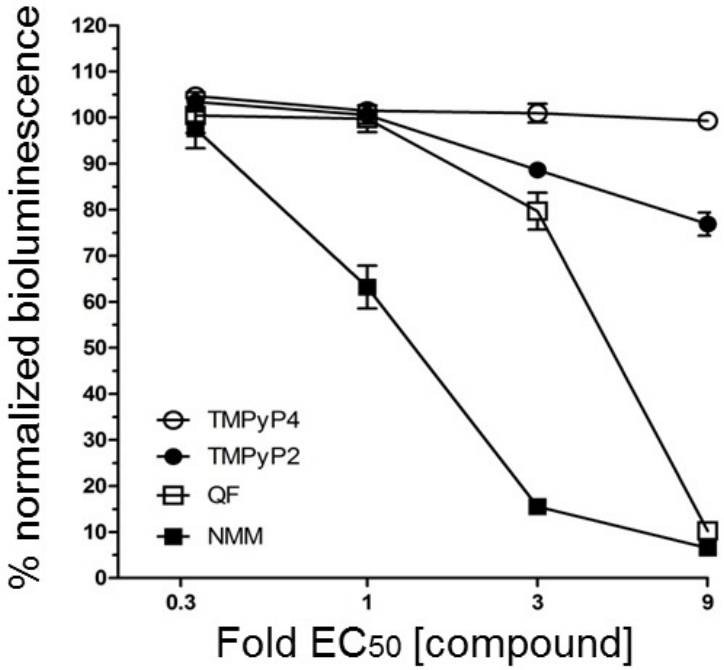

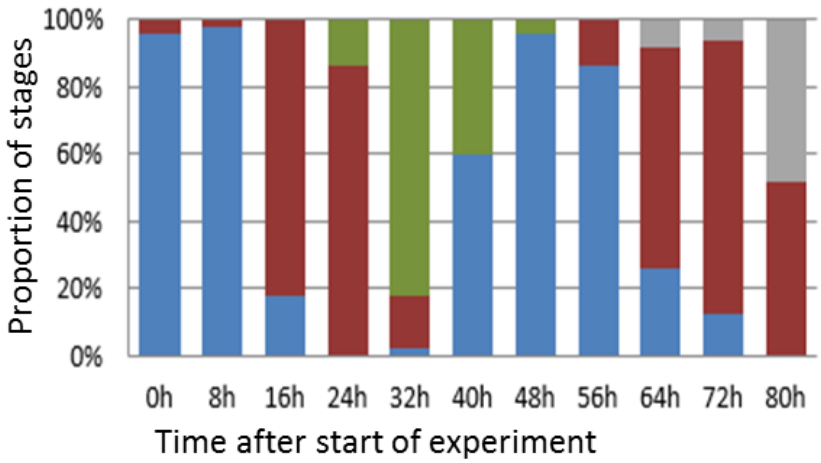

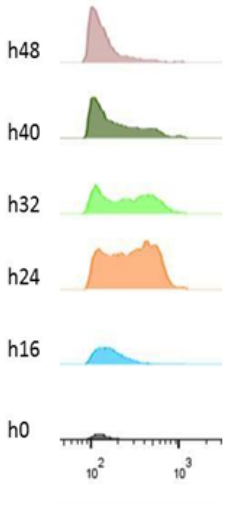

Control

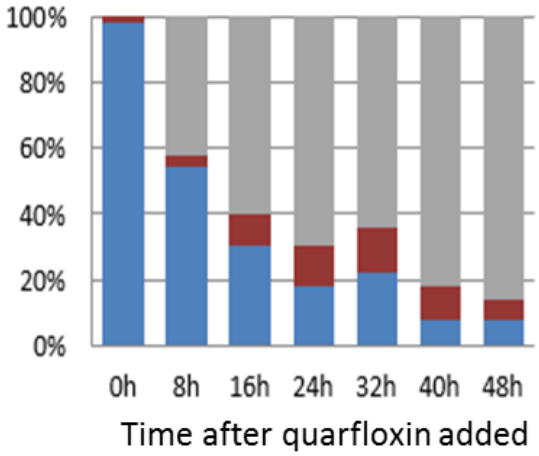

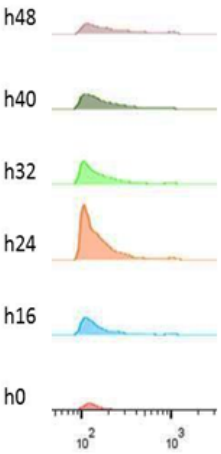

Quarfloxin added at rings (0 h)

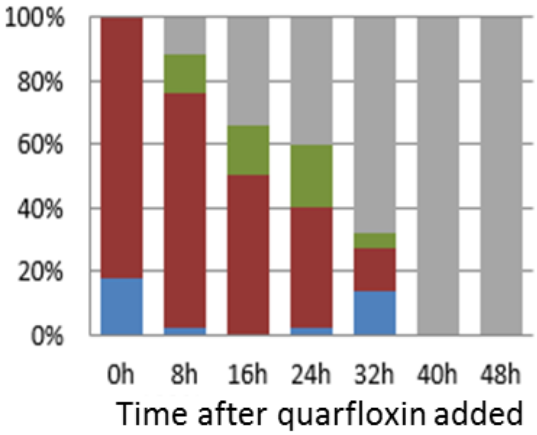

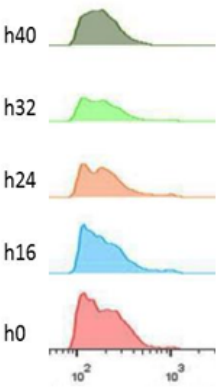

Quarfloxin added at trophozoites (16 h)

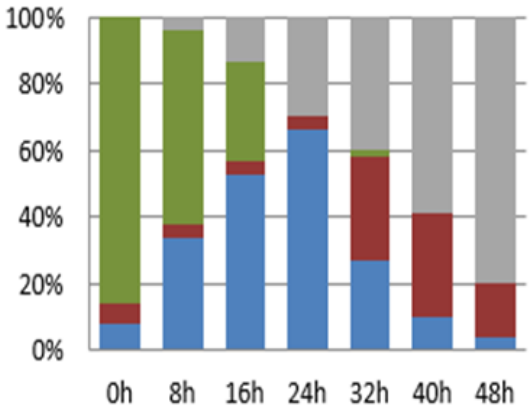

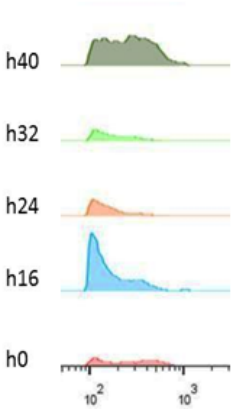

Quarfloxin added at schizonts (32 h)

A TTTGGGAGGGCTTGTTCCGGGAATGGGTT

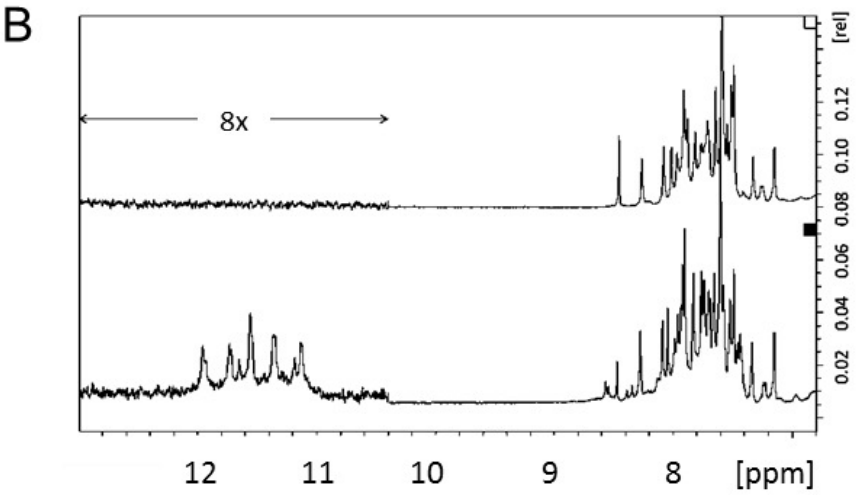

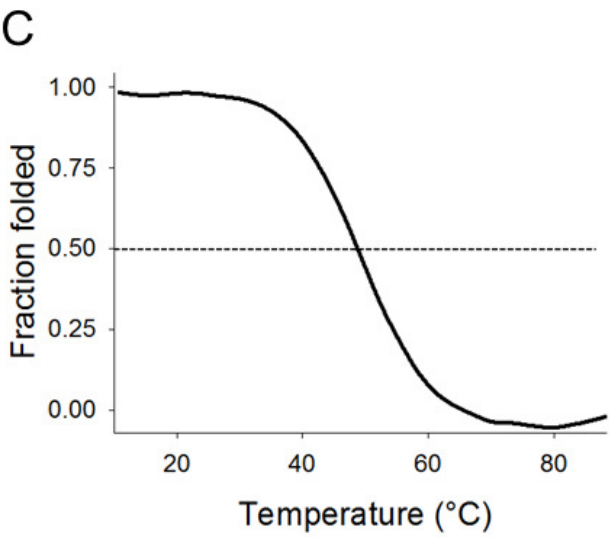

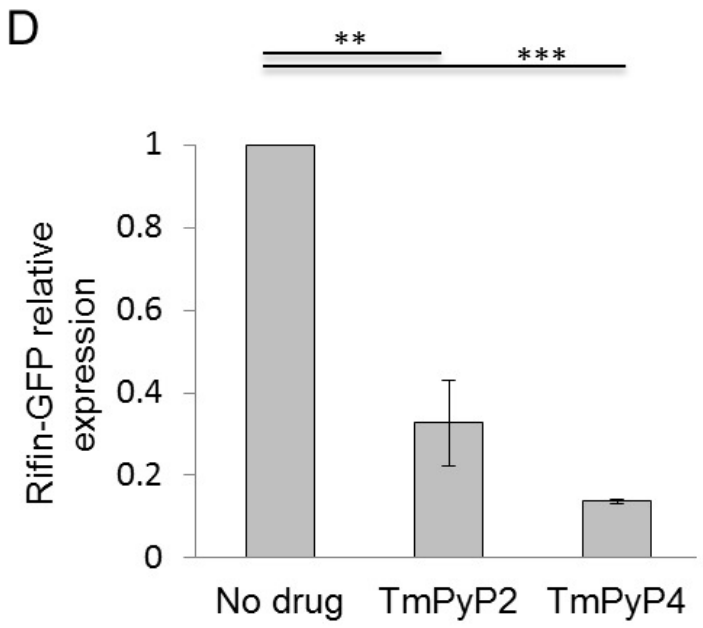

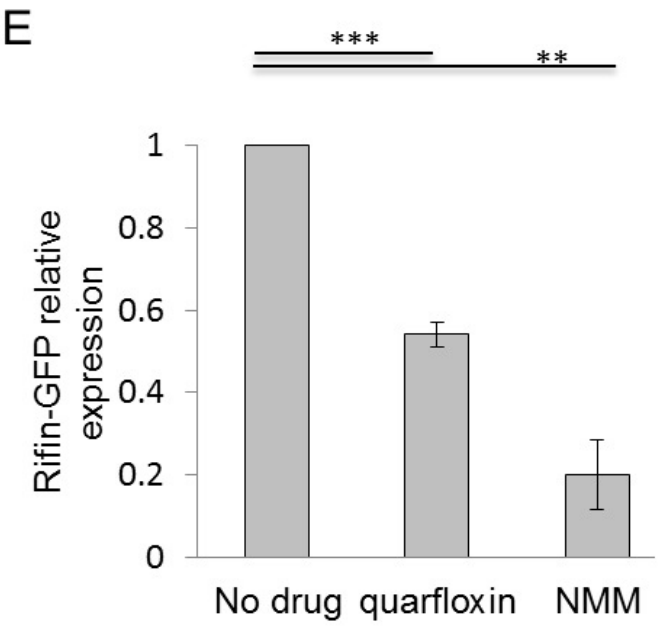

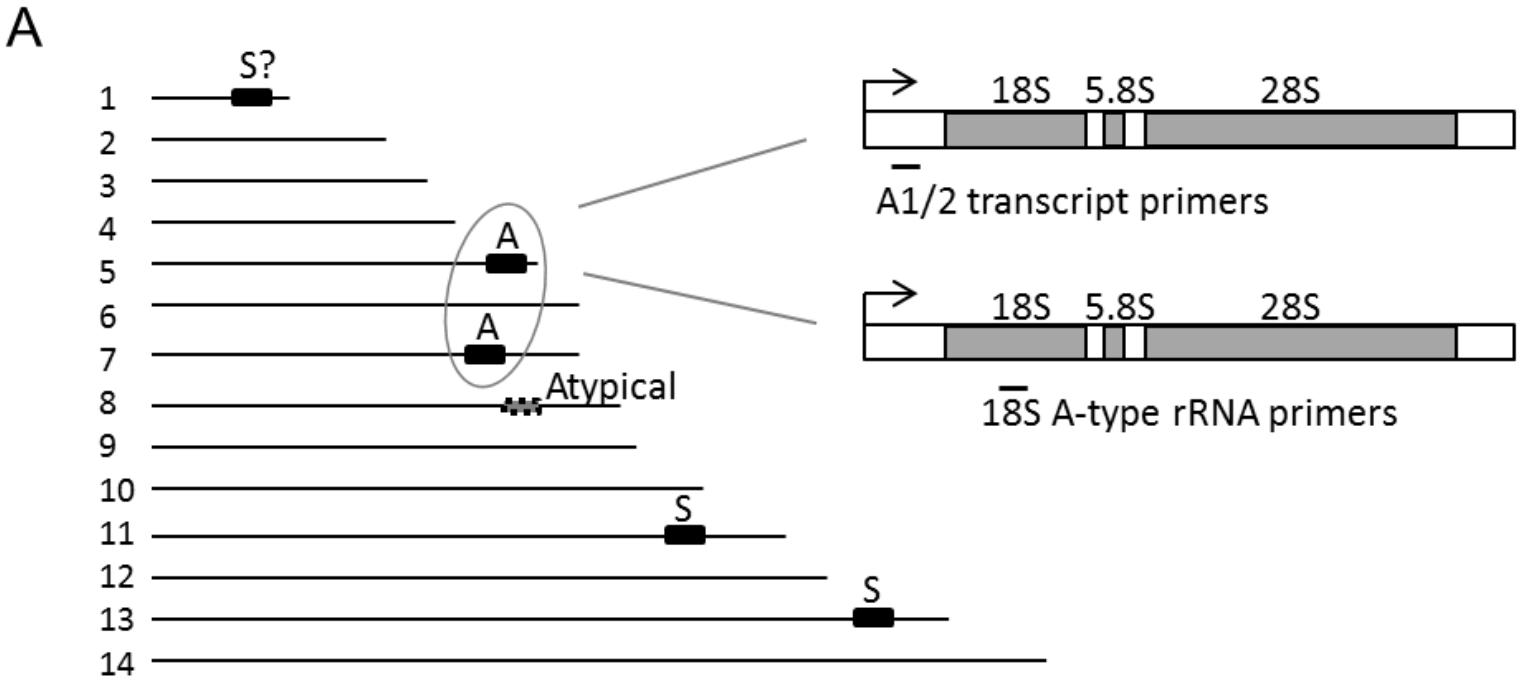
A
S?
1
2
3
4
5
6
7
8
9
10
11
12
13
14
A
A
Atypical
S
S
18S 5.8S 28S
A1/2 transcript primers
18S 5.8S 28S
18S A-type rRNA primers

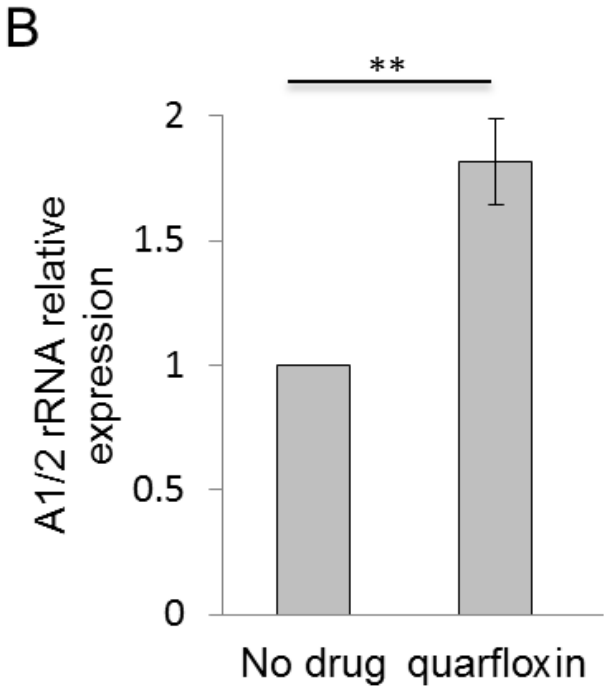
B
**
A1/2 rRNA relative expression
2
1.5
1
0.5
0
No drug
quarfloxin

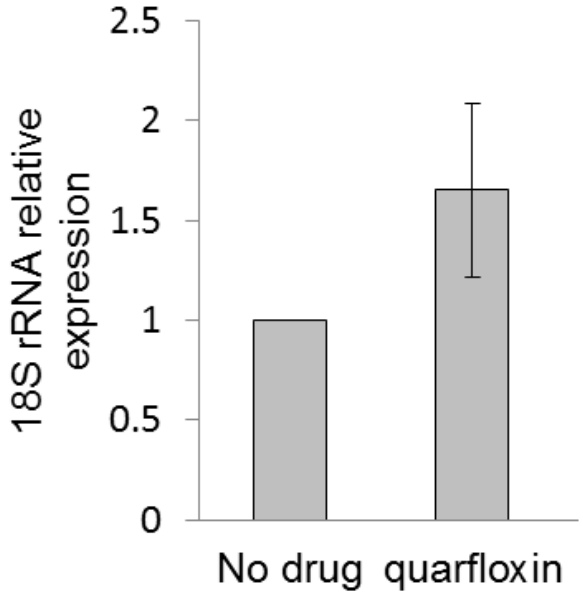
C
18S rRNA relative expression
2.5
2
1.5
1
0.5
0
No drug
quarfloxin